

# MULTI-HARMONIC ACCELERATING CAVITIES FOR RF BREAKDOWN STUDIES\*

Y. Jiang<sup>#</sup>, J. L. Hirshfield, Yale University, New Haven, CT 06511, USA

## Abstract

Multi-harmonic accelerating cavities that are explicitly designed for RF breakdown experiments are described. The fundamental  $TM_{010}$  and its higher harmonic  $TM_{011}$  or  $TM_{012}$  modes of the cavities are to be excited coherently by an external RF source in the expectation of lowering surface pulsed heating and/or surface electric field, so as to reduce breakdown probability and possibly achieve an increase in acceleration gradient.

## INTRODUCTION

In this paper, microwave cavities that support the superposition of the fundamental  $TM_{010}$  mode and at least one more mode whose eigen-frequency is a harmonic of the  $TM_{010}$  eigen-frequency are described. These bimodal cavities are explicitly intended to be vehicles that may deepen understanding of RF breakdown and pulsed heating, and as possible candidates for incorporation into multi-cavity high-gradient accelerator structures.

By selectively exciting synchronized multi-harmonic cavity modes driven externally in a precisely-controlled manner from a novel multi-frequency RF source available at Yale [1], unconventional spatiotemporal distributions of electromagnetic fields within a cavity can be realized, with the potential to lower field emission and/or pulsed heating at a given level of acceleration gradient; these effects are believed to be precursors to RF breakdown. In particular, two phenomena provide the main motivation for introduction of a 2<sup>nd</sup> mode at a harmonic frequency, namely: (a) the so-called anode-cathode effect [2]. In a longitudinally *asymmetric* cavity [2], phase-locked two-frequency operation, with the 2<sup>nd</sup> mode at a frequency double that of the fundamental, can allow the electric field pointing into one wall (cathode-like) to be significantly smaller than the field pointing out of that wall (anode-like), as shown in Fig. 1. A strong anode field will raise the work function barrier to suppress field and secondary emission; and (b) the suppression of pulsed heating, which is the focus of this paper. To model pulsed heating in a bimodal cavity, we characterize  $E$ -field superposition as  $E_{total} = (1 - \alpha)E_1 + \alpha E_2$ , where  $E_{1,2}$  is each electric field component with its associated acceleration gradient normalized to the same value, and  $\alpha$  is the percentage of the 2<sup>nd</sup> mode such that  $E_{total}$  provides the same acceleration gradient. Similarly, the surface RF  $H$ -field is  $H_{total} = (1 - \alpha)H_1 + \alpha H_2$ . Pulsed heating temperature rise  $\Delta T$  can then be approximately scaled in terms of  $H_1$  and  $H_2$  as  $\Delta T \propto (1 - \alpha)^2 < H_1^2 > + \alpha^2 \sqrt{f_2/f_1} < H_2^2 > = < H_1^2 > [(1 - \alpha)^2 + \alpha^2 \eta^2]$ , where

the frequency term  $\sqrt{f_2/f_1}$  is related to the ratio of surface resistivities,  $\eta = \sqrt{(f_2/f_1)^{1/2} < H_2^2 > / < H_1^2 >}$ , and the cross term averages out over one period. Due to the quadratic dependence of  $\Delta T$  upon  $\alpha$ , it is possible to choose an optimal  $\alpha$  such that  $(1 - \alpha)^2 + \alpha^2 \eta^2 < 1$ . In other words, to have lower temperature rise than for a single mode alone, while maintaining the same acceleration gradient; this is shown quantitatively in Fig. 1(b). The modified Poynting vector  $S_c$  [3], and total required RF power  $P_{tot}$ , also follow a quadratic dependence on the mode percentage  $\alpha$ , so use of two modes is expected to lower  $S_c$  and  $P_{tot}$  as well.

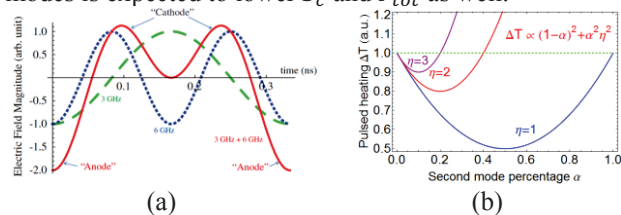


Figure 1: (a) Time dependence for a composite field (red line) excited at 3 GHz (green dashed) and 6 GHz (blue dotted), showing a factor-of-two anode-cathode field difference. (b) Dependence of the surface pulsed heating temperature rise  $\Delta T$  on the 2<sup>nd</sup> mode percentage  $\alpha$ . There is seen to be a range of  $\alpha$  within which  $\Delta T$  can be smaller than for a single mode (the green dashed horizontal line).

## $TM_{010} + TM_{011}$ CAVITY

For a simple pillbox designed as a bimodal cavity with a typical iris size of  $0.1\lambda - 0.2\lambda$  to support the  $TM_{010}$  mode and a 2<sup>nd</sup> harmonic  $TM_{011}$  mode, our analysis shows that  $\eta > 3$ . This implies that  $\Delta T$  could not decrease by more than 10% for a simple pillbox cavity. Consequently, a new software package is being developed by us to optimize cavity geometry to support multi-harmonic modes with desired RF properties, such as high shunt impedance and low surface fields, and maximize reduction in temperature rise  $\Delta T$ . This code integrates *Finite Element Method* and *Generic Algorithm*, so that it can find global optimization of RF parameters. Currently the code package is to include beam-cavity interactions that allow multipactor, wake field, and beam dynamics studies to be carried out in our unconventional structures, so as to provide a single software suite to expedite cavity design and optimization of RF properties and beam dynamics.

Optimization of design for a bimodal cavity supporting the  $TM_{010}$  mode and its 2<sup>nd</sup> harmonic  $TM_{011}$  mode can be realized using this code, as shown in Fig. 2. It is a full  $\pi$ -mode accelerating cavity, longitudinally symmetric with iris and beam pipe. Its fundamental frequency is at X-

\*Work supported by U.S. DOE

<sup>#</sup>yong.jiang@aya.yale.edu

band (12 GHz), to benchmark against the empirical criteria recently proposed within the worldwide High Gradient Collaboration: namely, a surface electric field  $E_{SUR}^{max} < 260 \text{ MV/m}$  and pulsed surface heating  $\Delta T^{max} < 56 \text{ K}$  in an X-band structure [4].

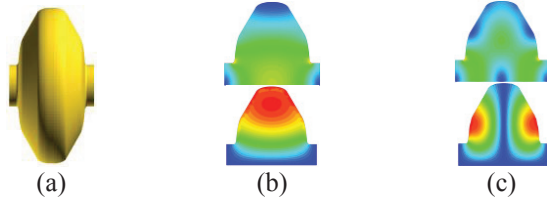


Figure 2: Field patterns in an optimized bimodal cavity (a) for the  $TM_{010}$  mode (b), and its 2<sup>nd</sup> harmonic  $TM_{011}$  mode (c). Top patterns are  $E$ -field, bottom are  $H$ -field.

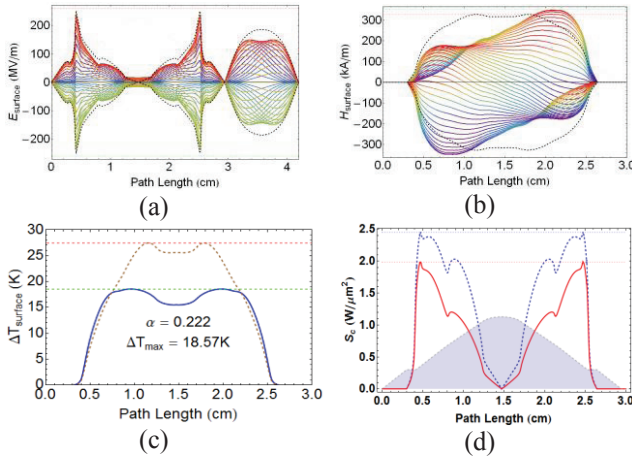


Figure 3: (a) Surface  $E$ -field and (b) surface  $H$ -field along the cavity periphery at different times for superposition of  $TM_{010}$  and  $TM_{011}$  modes, where the dotted line indicates fields of mode  $TM_{010}$  alone.  $H$ -field asymmetry is due to field distribution and chosen phase of the  $TM_{011}$  mode. (c) Optimized maximum pulsed heating temperature rise  $\Delta T$  (blue line) is 18.57 K, compared to that of single mode 27.5 K (brown dotted line), both for a 200 ns pulse width; (d) maximum modified Poynting vector  $S_c$  (red line) is  $1.95 \text{ W}/\mu\text{m}^2$  compared to a single mode value (blue dashed line) of  $2.45 \text{ W}/\mu\text{m}^2$ . The factor  $\alpha$  for the 2<sup>nd</sup> mode in this example is 0.222. The gray area in (d) indicates the stretched cavity profile.

With this optimized cavity profile, the benefits of reducing surface pulsed heating, modified Poynting vector, and total RF power are demonstrated, as shown in Fig. 3 and Table 1. In Fig. 3, the pulsed heating temperature rise for our 2-mode superposition can be 32% smaller than that for the fundamental mode alone for the same cavity; and the maximum modified Poynting vector  $S_c$  can be lower by 20%, with a 22% 2<sup>nd</sup> harmonic component and a relative phase between the two modes of 90° (both modes are in sychromization should this bimodal cavity be operated in an accelerating structure). The peak surface  $E$ -field is the same as that of the fundamental mode due to this phase relationship, and no anode-cathode effect is present. Note, that even for a

single  $TM_{010}$  mode,  $S_c$  is small due to the reduced  $H$ -field around the iris as a result of optimization. In Table 1, RF parameters of this bimodal cavity are listed in comparison with other cavity configurations. Although the instantaneous surface  $H$ -field is increased, the pulsed heating temperature rise is lowered since the exposure time to the peak  $H$ -field is shortened, and temperature rise is a time-averaged effect quadratically dependent on the mode percentage  $\alpha$  in our 2-mode superposition. The total RF power is reduced, while maintaining the same acceleration gradient, so its effective shunt impedance is significantly increased.

### TM<sub>010</sub> + TM<sub>012</sub> CAVITY

Because of different magnitudes and profiles of field distributions along the cavity walls for different modes in bimodal cavities, it is possible to have partial electric field cancellation on walls so that the maximum surface  $E$ -field can be smaller than that of single mode. We have analysed a  $\pi$ -mode accelerating cavity shown in Fig. 4 that supports the  $TM_{010}$  mode and its 3<sup>rd</sup> harmonic  $TM_{012}$  mode. When both modes reach the peak axial accelerating fields synchronously, the  $TM_{012}$  mode has its surface electric field opposite in direction to that of the fundamental  $TM_{010}$  mode on the side walls, and hence lowers the surface electric field significantly, as shown in Fig. 5. Preliminary analyses show that reductions in the maximum pulsed heating temperature rise of up to 21.5%, of the modified Poynting vector by 29.5%, peak surface  $E$ -field by 19.4%, total RF power by 18.9% are predicted for this bimodal cavity, than those for single mode operation at the same acceleration gradient for the same cavity. Also, its effect shunt impedance of  $124.2 \text{ M}\Omega/\text{m}$  is larger by 23.3%.

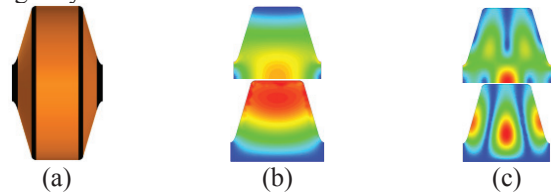






Figure 4: (a) Optimized bimodal cavity profile, with  $a/\lambda = 0.1$ . Field patterns for the  $TM_{010}$  mode (b), and its 3<sup>rd</sup> harmonic  $TM_{012}$  mode. Top patterns are  $E$ -field, bottom are  $H$ -field.

### RF BREAKDOWN STUDY

It is of obvious interest to measure RF breakdown statistics for these bimodal cavity designs, comparing single mode and 2-mode superposition, and to investigate surface fatigue on cavity surfaces after pulsed heating. An RF breakdown study is to be carried out based on availability in the Yale Beam Physics Lab of a unique 2-frequency phase synchronous RF source at S-band (2.856 GHz) and its higher harmonics, either at C-band (5.712 GHz) or X-band (8.856 GHz). The 2-frequency RF source will provide mutually phase-locked multi-MW  $\sim 1 \mu\text{s}$  pulses at both fundamental and higher harmonic

Table 1: Comparison of RF parameters between an optimized bimodal  $TM_{010}+TM_{011}$  cavity and single mode cavities, where effective acceleration gradient is equalized at 100 MV/m, with red/green arrows showing up/down improvements. Pillbox A has the same maximum surface  $H$ -field as that of the fundamental mode in bimodal cavity; Pillbox B the same maximum surface  $E$ -field; and the nose-cone cavity is a single-mode cavity optimized to increase shunt impedance and lower surface pulse heating using the same code.

$a/\lambda=0.12$ $\pi$ mode standing wave effective gradient $E_a = 100MV/m$	 $TM_{010}+TM_{011}$ Bimodal Cavity			 Pillbox A	 Pillbox B	 Nose-cone
	1 <sup>st</sup> harmonic alone	2 <sup>nd</sup> harmonic alone	78% 1 <sup>st</sup> +22% 2 <sup>nd</sup>	1 <sup>st</sup> harmonic only	1 <sup>st</sup> harmonic only	1 <sup>st</sup> harmonic only
frequency (GHz)	11.9942	23.9884		11.9942	11.9942	11.9942
effective shunt impedance (M $\Omega$ /m)	95.7	38.3	$\blacktriangle 131.4$	89.7	99.1	113.9
transit time factor	0.765	0.786		0.768	0.753	0.758
max $E_{surf}$ (MV/m)	246.8	367.4	246.8	209.7	246.8	225.0
max $H_{surf}$ (MA/m)	0.327	0.634	0.350	0.327	0.298	0.289
max $S_c$ ( $W/\mu m^2$ )	2.45	10.3	$\blacktriangledown 1.95$	3.75	3.02	4.20
max $\Delta T$ (K) @ 200ns pulse length	27.5	148.2	$\blacktriangledown 18.6$	27.5	22.87	21.5
wall loss (MW)	1.306	3.263	$\blacktriangledown 0.95$	1.392	1.262	1.097

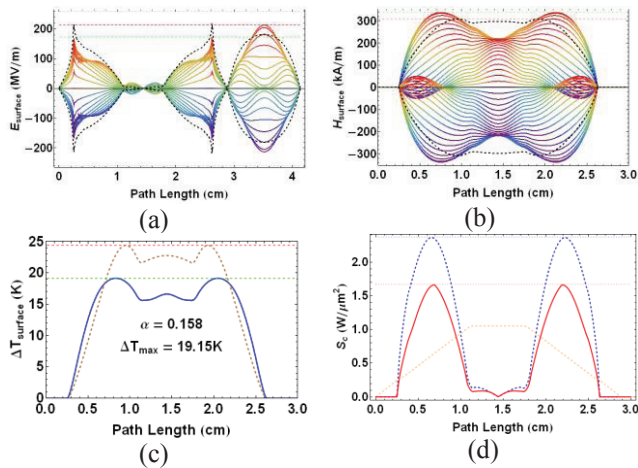


Figure 5: (a) surface  $E$ -field and (b) surface  $H$ -field along the cavity periphery at different times for superposition of  $TM_{010}$  and  $TM_{012}$  modes, where the dotted line indicates fields of single mode  $TM_{010}$ . (c) Optimized maximum pulsed heating temperature rise (blue line) is 19.15 K, compared to that of single mode 23.7 K (brown dotted line) with a 200 ns pulse width; (d) the maximum modified Poynting vector  $S_c$  (red line) is  $1.67 W/\mu m^2$  compared to a single mode value (blue dashed line) of  $2.37 W/\mu m^2$ .  $\alpha$  for the 2nd mode is 0.158.

frequencies with continuously-adjustable amplitudes and relative phase difference. The cavity geometry suitable for RF breakdown tests at Yale using S-band (2.856 GHz) as the fundamental frequency can be directly scaled from the optimized geometries shown above. RF breakdown tests in travelling wave or standing wave single cell structures [5] can be devised to benchmark with the existing RF breakdown data [3]. With better understanding of RF breakdown physics supported by

experimental evidence and further development of computational tools, design concepts for accelerator structures comprising multi-harmonic cavities will be developed.

Bimodal cavities with the necessary tight dimensional tolerances require meticulous machining; but should be possible using recently described techniques that maintained dimensions to within 5  $\mu m$  [6]. Further evidence for precision tuning of a not-dissimilar bimodal cavity has also been reported [1].

## CONCLUSION

This paper describes use of multi-harmonic cavities powered by a dual frequency RF source to systematically study mechanisms which seem likely to influence the onset of RF breakdown. It is anticipated that deepened understanding of these mechanisms could lead to improved design of accelerator structures with higher shunt impedance, higher accelerator gradient, and lower breakdown probability than can be built at present.

## ACKNOWLEDGMENT

The authors would like to thank Professor R.M. Jones from Manchester Univ. (UK) for valuable discussions.

## REFERENCES

- [1] Y. Jiang, et al, NIM A, v657, pp 71-77 (2011).
- [2] S.V. Kuzikov et al, Phys. Rev. Lett. 104, 214801 (2010).
- [3] A. Grudiev, et al, Phys. Rev. ST Accel. Beams, 12, 102001 (2009); and citations therein.
- [4] A. Grudiev, et al, Proceedings of LINAC08, Victoria, Canada THP062, pp.923-935 (2008).
- [5] V.A. Dolgashev, et al, SLAC-PUB-10667 (2004).
- [6] S. Atieh, et al, IPAC2011, pp. 1768-1770 (2011).